TISSUE ENGINEERING: Part C
Volume 22, Number 11, 2016

DOI: 10.1089/ten.tec.2016.0106

termis
Tissue Engineering
& Regenerative Medicine
International Society

METHODS ARTICLE

Development and Validation of Noninvasive Magnetic Resonance Relaxometry for the *In Vivo* Assessment of Tissue-Engineered Graft Oxygenation

Samuel A. Einstein, PhD,[1] Bradley P. Weegman, PhD,[1] Meri T. Firpo, PhD,[2] Klearchos K. Papas, PhD,[3] and Michael Garwood, PhD[1]

Techniques to monitor the oxygen partial pressure (pO_2) within implanted tissue-engineered grafts (TEGs) are critically necessary for TEG development, but current methods are invasive and inaccurate. In this study, we developed an accurate and noninvasive technique to monitor TEG pO_2 utilizing proton (^1H) or fluorine (^{19}F) magnetic resonance spectroscopy (MRS) relaxometry. The value of the spin-lattice relaxation rate constant (R_1) of some biocompatible compounds is sensitive to dissolved oxygen (and temperature), while insensitive to other external factors. Through this physical mechanism, MRS can measure the pO_2 of implanted TEGs. We evaluated six potential MRS pO_2 probes and measured their oxygen and temperature sensitivities and their intrinsic R_1 values at 16.4 T. Acellular TEGs were constructed by emulsifying porcine plasma with perfluoro-15-crown-5-ether, injecting the emulsion into a macroencapsulation device, and cross-linking the plasma with a thrombin solution. A multiparametric calibration equation containing R_1, pO_2, and temperature was empirically generated from MRS data and validated with fiber optic (FO) probes *in vitro*. TEGs were then implanted in a dorsal subcutaneous pocket in a murine model and evaluated with MRS up to 29 days postimplantation. R_1 measurements from the TEGs were converted to pO_2 values using the established calibration equation and these *in vivo* pO_2 measurements were simultaneously validated with FO probes. Additionally, MRS was used to detect increased pO_2 within implanted TEGs that received supplemental oxygen delivery. Finally, based on a comparison of our MRS data with previously reported data, ultra-high-field (16.4 T) is shown to have an advantage for measuring hypoxia with ^{19}F MRS. Results from this study show MRS relaxometry to be a precise, accurate, and noninvasive technique to monitor TEG pO_2 *in vitro* and *in vivo*.

Keywords: ^{19}F-MRS, oximetry, tissue-engineered graft, relaxometry, islet transplantation, oxygen measurement

Introduction

Tissue-engineered grafts (TEGs) have the potential to treat numerous devastating diseases including type 1 diabetes.[1–6] Pancreatic islet transplantation is a potential treatment for type 1 diabetes, but favorable long-term outcomes are inconsistent because intrahepatic delivery of islets is not optimal.[6–10] Additionally, current demand for donor pancreata far exceeds supply and allotransplantation requires a lifetime of immunosuppression.[7,9,10] Macroencapsulated TEGs may ameliorate or eliminate these limitations by allowing the use of alternative cell sources (such as porcine or stem cell-derived islets) and providing an immunoisolating membrane.[1–6]

Macroencapsulation of islets within a TEG offers many advantages; however, oxygenation is a critical limitation for the development of large-scale and high-cell density implanted TEGs.[11] Noninvasive monitoring of the oxygen partial pressure (pO_2) within TEGs is critically important because of the deleterious effects of long- and short-term exposure of islet tissue to hypoxia or anoxia.[2,7,8,11–13] Lack of oxygen is the most critical issue preventing widespread utilization of macroencapsulated islet transplantation, and delivery of exogenous oxygen has been shown to enhance TEG survival and function *in vivo*.[2,14,15] Noninvasive monitoring of pO_2 can improve TEG development and allow the evaluation of TEG viability[16] and local changes in

[1]Department of Radiology, Center for Magnetic Resonance Research, University of Minnesota, Minneapolis, Minnesota.
[2]Department of Medicine, Stem Cell Institute, University of Minnesota, Minneapolis, Minnesota.
[3]Department of Surgery, University of Arizona, Tucson, Arizona.

pO_2 with the delivery of supplemental oxygen (DSO). Oxygen measurements are especially important in TEGs that have not revascularized due to either lack of time or the presence of an immunoisolating membrane. Additionally, pO_2 measurements may detect oxygenation-altering events such as cell proliferation, inflammation (including fibrous capsule formation), and vascularization.[17]

Eppendorf needle probes utilizing polarographic techniques remain the gold standard for *in vivo* oxygen measurements.[18,19] These needle probes, however, are invasive, magnetic resonance (MR)-unsafe, and only measure the oxygen at a single point necessitating multiple measurements to map the average oxygenation of a given volume. Additionally, these probes may consume oxygen during operation and may introduce oxygen to the system during the mechanically invasive measurement procedure. Luminescence-based fiber-optic (FO) sensors are an MR-compatible oxygen-measurement technique providing equivalent results when compared with Eppendorf probes while remaining invasive and limited to single-point measurements.[20] Optical and photoacoustic lifetime-imaging techniques remain applicable only to superficial oxygen measurements.[19,21,22] Nuclear medicine techniques require the injection of radioactive tracers, often require an on-site accelerator, and the results remain difficult to quantify.[18,19,23]

Magnetic resonance spectroscopy (MRS) allows for noninvasive, real-time, aggregate oxygen measurements *in vivo*. The spin-lattice relaxation rate constant (R_1) is sensitive to oxygen concentration as a result of dipole–dipole interactions between the nucleus and the unpaired electrons in the dissolved oxygen gas.[18,24,25] Because R_1 is sensitive to oxygen concentration rather than pO_2, R_1 measurements are independent of gas solubility, but can easily be converted to pO_2 values using Henry's law.[26] Perfluorinated compounds (PFCs) are commonly used as MRS oxygen probes because of their high oxygen solubility and hydrophobic nature.[25,26] The hydrophobicity prevents the R_1 of such compounds from being influenced by confounding factors *in vivo* such as variable ion concentrations or pH. The most prevalent and promising PFC probes found in literature include perfluoro-15-crown-5-ether (PFCE), hexafluorobenzene (HFB), perfluorodecalin (PFD), perfluorooctyl bromide (PFOB), and perfluorotributylamine (PFTBA).[24,25,27–40] Hexamethyldisiloxane (HMDSO), a ^{1}H probe, has shown promise as well.[37,41]

MRS methods utilizing these probes have been used to both measure and image oxygen *in vivo*, but have had limited clinical applications due to large measurement errors and difficulty with molecule delivery to target tissues. Both the R_1 and oxygen sensitivity (change in R_1 for a given change in pO_2 at a specified temperature) of the MRS probes are affected by temperature and static magnetic field strength making a proper calibration critical to minimizing pO_2 measurement error. This study used temperature-compensating multiparametric calibrations to reduce measurement error.[27] Additionally, most previous ^{19}F-MRS oximetry studies evaluated PFCs directly injected into the tissue of interest[37,40] or intravenously into tumors that often have chaotic and ineffective vasculature,[27,28,30,31,34,35] which resulted in inhomogeneous distributions of the probes. An additional benefit of measuring pO_2 within TEGs, therefore, is the removal of limitations due to ineffectual probe delivery.

Previous studies have successfully measured the pO_2 of encapsulated cell systems *in vivo*. PFC-loaded alginate beads implanted into the rodent kidney capsule, peritoneal cavity, and quadriceps femoris muscle reveal a hypoxic environment unconducive to islet survival.[38,42–44] Macroencapsulated cell systems, however, are often implanted into the subcutaneous space[2] and these studies, limited to microencapsulation, did not examine the oxygen availability of this site.

In this study, we first measured the oxygen and temperature sensitivities of several MRS oxygen probes to choose the most appropriate probe for our application. We then developed MRS techniques to measure encapsulated TEG pO_2 *in vitro* and implanted into a subcutaneous pocket of a rat *in vivo*. Additionally, both techniques were validated with FO pO_2 probes. Finally, we demonstrated that changes in TEG pO_2 resulting from DSO can be monitored with our MRS relaxometry technique.

Materials and Methods

^{19}F and ^{1}H R_1 measurement

^{19}F-MRS spectra were acquired with a 16.4 T MR system (Agilent Technologies, Santa Clara, CA) using a custom-built single-loop surface coil tuned to 656.8 MHz. For HMDSO, the coil was tuned to ^{1}H (698.2 MHz). A standard inversion-recovery pulse sequence was used to measure R_1. Adiabatic half-passage (90°) and inversion (180°) pulses were used to ensure uniform flip angles. For each scan, the magnetization recovery was interrogated after various delay times. Single spectra were acquired for *in vitro* experiments, but *in vivo* data were averaged ($N=2$) to increase the signal-to-noise ratio (SNR) and reduce errors. The unapodized spectra were processed by automatically correcting the phase, baseline, and drift using VnmrJ (Agilent Technologies). The peaks were then integrated and the peak areas were fit to Equation (1) using a three-parameter nonlinear regression with GraphPad Prism (v5; GraphPad Software, Inc., La Jolla, CA). Equation (1) is the solution to the Bloch equation for the longitudinal magnetization (M_z) during an inversion-recovery pulse sequence when repetition time (TR) $>>T_1$ and echo time $<<T_2$, where α and β are fitting constants and t is the recovery time. The additional fitting constant was utilized because it can compensate for imperfect inversion and has been previously and successfully applied to ^{19}F relaxometry.[27,34,35,42,44]

$$M_z = \alpha \cdot \left(1 - 2e^{-R_1 \cdot t}\right) + \beta \quad (1)$$

PFC and HMDSO MRS calibration

Various probes were tested for oxygen and temperature sensitivity using neat compounds. To calibrate each PFC (PFCE [Exfluor Research Corporation, Round Rock, TX], HFB [Sigma-Aldrich, St. Louis, MO], PFD [Fluoromed, L.P, Round Rock, TX], PFOB [Sigma-Aldrich], PFTBA [Sigma-Aldrich]), and HMDSO (Sigma-Aldrich), 1.8 mL of the selected molecule was placed into a 2 mL vial. The vial was placed in the center of the surface coil; the coil was tuned, and inserted into the magnet. PFCE, HFB, and HMDSO benefit from processing only a single resonance. For PFD, PFOB, and PFTBA (which have multiple resonances), the I-,[45] θ-,[29] and δ-[29] resonances, respectively, were interrogated. The sample was then bubbled with a gas of known oxygen concentration for 30 min while the temperature was held constant. The

magnet was shimmed and R_1 was then measured as described above and delay times were optimized to each sample's R_1.[46,47] Measurements were made for five different pO_2s (0, 38, 76, 114, and 160 mmHg) at three different temperatures (21, 37, and 45°C). An FO temperature probe (SA Instruments, Inc., Stony Brook, NY) verified the temperature of the sample. Each condition was measured in replicate ($N=2$–6) with a TR of at least $5/R_1$. The R_1 was assumed to be a function of the pO_2, temperature (T), and four fitting constants [A, B, C, and D; Eq. (2)] as previously described.[27] This model accounts not only for the dipolar interactions of the dissolved oxygen gas, but for the effects of temperature on the correlation time and dissolved oxygen concentration as well. Fitting constant A is a result of dipole–dipole interactions between the magnetic moments of the nuclei of the probes (the most significant energy-transfer mechanism leading to relaxation in the anoxic probes). Fitting constant B is attributable to additional dipole–dipole interactions between the nuclei of the probes and the unpaired electrons of the dissolved oxygen gas, which quickens relaxation. Temperature alters the correlation time (the time scale on which these magnetic field fluctuations occur) and necessitates fitting constant C. Fitting constant D is due to cross-interactions of oxygen and temperature, mainly the temperature dependence of the Henry constant. Many of the physical processes associated with the fitting constants are complex, but yield a surprisingly linear relationship for the temperatures and pO_2s typically encountered during *in vivo* experiments.[27] R_1 measurements were fit to the multiparametric calibration equation using a Levenberg–Marquardt algorithm (OriginLab, Northampton, MA).

$$R_1 = A + B \cdot pO_2 + C \cdot T + D \cdot pO_2 \cdot T \tag{2}$$

TEG construction

TEGs were prepared by loading a macroencapsulation device with an oxygen-sensitive matrix. PFCE was chosen for the probe because of its high oxygen sensitivity, high nuclear molarity (equivalent nuclei per volume), and excellent reported biocompatibility.[32,40] Fluorine-loaded fibrin gels were prepared with 75 μL of porcine plasma (Sigma-Aldrich) emulsified with 75 μL of PFCE. The mixture was emulsified by manual agitation, injected into a 40 μL immunoisolation device (TheraCyte, Inc., Laguna Hills, CA) using a 250-μL precision syringe (Hamilton Company, Reno, NV), and then cross-linked with 5% v/v bovine thrombin solution. The thrombin solution was made by diluting concentrated topical thrombin solution (GenTrac, Inc., Middleton, WI) in phosphate-buffered saline with calcium and magnesium (PBS++) (Gibco, Thermo Fisher Scientific, Waltham, MA). The cell access port was trimmed short, and sealed with adhesive (Dermabond; Ethicon, Inc., Somerville, NJ).

^{19}F-MRS TEG calibration

TEGs were prepared as described above and placed into a 50 mL conical tube filled with PBS++. An FO oxygen probe (Ocean Optics, Dunedin, FL) was inserted into the TEG for simultaneous comparison with ^{19}F-MRS-measured pO_2. The vial was placed in the center of the coil; the coil was tuned, and inserted into the magnet. The sample was then bubbled with a gas of known oxygen concentration for 30 min while the temperature was held constant. The magnet was shimmed and R_1 was then measured as described above with 10 different delay times (0.05, 0.1, 0.15, 0.25, 0.5, 0.75, 1, 2, 4, and 5 s). Measurements were made for five different pO_2s (0, 38, 76, 114, and 160 mmHg) at three different temperatures (21, 37, and 45°C) as verified with the FO temperature probe as described above. Each condition was measured in replicate ($N=6$) with a TR of 6 s. The R_1 was again fit to the multiparametric calibration equation using a Levenberg–Marquardt algorithm.

TEG implantation

All animal research was approved and overseen by the University of Minnesota Institute for Animal Care and Use Committee (IACUC). A total of nine male Lewis rats were implanted with a PFCE-loaded TEG. On the day of implantation, rats were anesthetized with inhalation isoflurane using a respirator and vaporizer. The surgical sites were shaved with an electric clipper, and the skin was surgically prepped with chlorhexidine or equivalent antiseptic. A 1.5 cm incision was made in the skin on the dorsal side, just inferior to the scapulae, and perpendicular to, but symmetric across the medial line. Using gentle blunt dissection, a small pocket was created adjacent to the vertebral column just large enough to accommodate the device snugly. The pocket was rinsed and lubricated with saline, and the device was tucked into the pocket. The device was completely fabricated using plastic (PTFE) materials, designed for flexibility and biocompatibility. The incision was closed with absorbable suture in a normal fashion using at least two layers and taking care to make sure the device components were not directly below the incision. Surgical glue was applied over the closed incision as a barrier. NSAIDs (meloxicam, 1 mg/kg) were administered by subcutaneous injection to minimize pain and inflammation for three or more days following surgery. Animals were monitored daily during recovery for up to 14 days until the incision was fully healed.

In vivo *oximetry in rats*

The subcutaneous TEG pO_2 of six rats was evaluated 1, 4, 8, 15, 22, and 29 days postimplantation. On the day of measurement, rats were anesthetized with inhalation isoflurane, immobilized onto a holder with the device centered over the custom-built surface coil, stabilized at a core body temperature of 37°C ± 0.2°C as measured with a rectal thermocouple, and inserted into the 16.4 T horizontal-bore magnet. Animals were continuously monitored during scanning with anesthesia depth and forced-air heater temperature adjusted as needed. After the coil was tuned and the magnet shimmed, R_1 measurements ($N=6$) were made with the inversion-recovery sequence with adiabatic pulses used for TEG calibration. The R_1 of each measurement was then converted to a pO_2 using the multiparametric calibration previously determined *in vitro*. Following completion of the study, animals were promptly euthanized using CO_2 for device explant and gross evaluation.

Validation of ^{19}F-MRS in vivo pO_2 measurements

The ^{19}F-MRS pO_2 measurements of a subset of TEGs ($N=3$) were validated with an FO probe *in vivo*. These

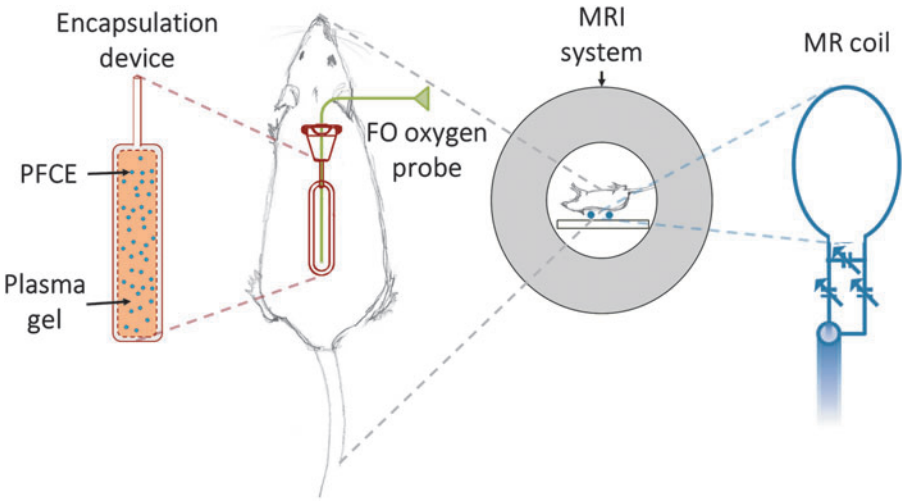

FIG. 1. Illustration of a macroencapsulation device with access port (*red*) in a dorsal subcutaneous pocket of a Lewis rat. For FO measurements, the 250-μm thin-fiber oxygen probe (*green*) was inserted transcutaneously through the skin and access port into the cell compartment of the device. The ^{19}F-MRS coil (*blue*) was placed on the dorsal side of the anesthetized rat to detect the ^{19}F signal of the PFCE within the device. FO, fiber optic; MRS, magnetic resonance spectroscopy.

devices were equipped with an additional access port (In-Line access port; Access Technologies, Skokie, IL). On the day of scanning, rats were anesthetized and a transcutaneous catheter was inserted into the access port. A previously calibrated ultra-thin 250 μm FO probe (Ocean Optics) was then threaded through the catheter into the TEG and the rat was inserted into the MR system (Fig. 1). FO pO_2 was measured simultaneously with the MRS pO_2 measurement technique for direct comparison.

TEGs with DSO

A small group of rats ($N=3$) were acclimated with a harness and tether apparatus (Instech Laboratories, Plymouth Meeting, PA) for 2 weeks before implantation with a TEG modified for DSO. The harness and tether apparatus contains a swivel, and counter-balance system to allow for animal movement around the cage, and normal feeding, drinking, and grooming behaviors. The TEGs were modified to include an internal compartment and cannulae for transcutaneous oxygen delivery *in vivo.* Briefly, two additional internal membranes were added to the macroencapsulation device previously described to create a three-chamber device with an internal oxygen compartment, and two distinct cell compartments superior and inferior to this central oxygen compartment. Further, three additional access ports were added to the device to allow access to each compartment. Two access ports provided access to the central compartment to allow for oxygen gas infusion and effusion while two additional ports provided access to the superior and inferior cell compartments. TEGs for DSO were prepared by loading the cell compartments of the modified devices with the acellular PFCE-plasma gel emulsion described above.

The TEGs were then implanted in the subcutaneous space as described above leaving the oxygen compartment access cannulae protruding through the incision for attachment to the harness and tether apparatus. The tether system was connected through the cage lid to an electrochemical oxygen generator (Giner, Inc., Newton, MA) through a specialized manifold to regulate and monitor the delivery of oxygen gas to the implanted devices. Pure humidified oxygen gas (760 mmHg) was continuously delivered through the harness and tether apparatus to the modified TEG for the duration of the study. Extended sections of tubing were used to continue DSO during pO_2 assessment, which was measured with ^{19}F-MRS 1 day postimplantation. DSO was then discontinued for 1 day and the pO_2 of the TEG was reassessed with ^{19}F-MRS. R_1 measurement and conversion to pO_2 was as described above except for the addition of a 760 mmHg pO_2 to the calibration procedure.

Comparative data collection and analysis

A thorough review of literature was conducted to allow a comparison of our findings and determine whether the static magnetic field strength (B_0) affects R_1 oxygen sensitivity,

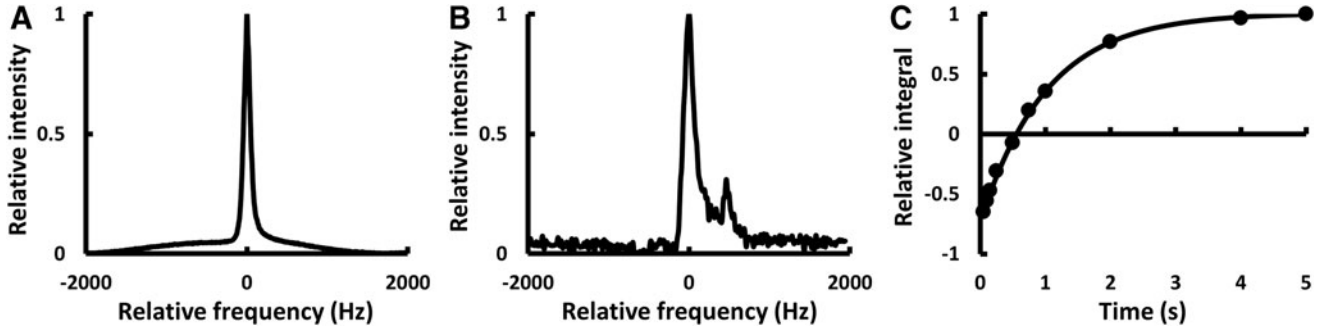

FIG. 2. Typical ^{19}F-MRS spectra from PFCE within an immunoisolation device **(A)** *in vitro* (SNR = 529; FWHM = 91 Hz) and **(B)** *in vivo* (SNR = 40.5; FWHM = 157.8 Hz). **(C)** The fitted inversion-recovery curve from the experiment that produced the *in vivo* spectrum ($\alpha = 0.861$; $\beta = 0.146$; $R_1 = 0.985\ s^{-1}$). FWHM, full width at half maximum; SNR, signal-to-noise ratio.

Table 1. Results of the Calibration of the PFCs and HMDSO Revealed Differences in pO_2 Sensitivity at 37°C, Anoxic Temperature Sensitivity, and Anoxic R_1 at 37°C Between the Different Probes

Probe	*Equivalent nuclei*	*Nuclear molarity (M)*	*pO_2 sensitivity*[a] *(10^{-5} $mmHg^{-1}\cdot s^{-1}$)*	*Temperature sensitivity*[b] *(10^{-4} $°C^{-1}\cdot s^{-1}$)*	*R_1,*[a,b] *(s^{-1})*
PFCE	20	61	223.4 ± 15	−197.4 ± 2.5	0.943 ± 0.014
HFB	6	52	133.2 ± 18	−41.90 ± 2.7	0.388 ± 0.015
PFD-I	2	8	188.0 ± 38	−76.90 ± 6.4	0.271 ± 0.031
PFOB-θ	3	12	199.6 ± 6.8	−106.1 ± 1.4	0.657 ± 0.007
PFTBA-δ	9	25	226.0 ± 78	−289.9 ± 16	1.551 ± 0.080
HMDSO	18	85	101.1 ± 11	−3.013 ± 2.1	0.116 ± 0.011

[a]37°C.
[b]Anoxia.
PFCs, perfluorinated compounds; pO_2, oxygen partial pressure.

R_1 temperature sensitivity, or anoxic R_1 of PFCE. Data were collected from relevant publications identified using electronic databases (PubMed and Google Scholar) and references cited in relevant publications. Data collected included B_0, change in PFCE R_1 with oxygen concentration, change in PFCE R_1 with temperature, and PFCE anoxic R_1. Results were excluded if any information other than change in PFCE R_1 with temperature was not available. It was assumed that creating an emulsion with PFCE does not change its relaxation. After compilation, data were fitted assuming a linear relationship between B_0 and the parameters of interest. These fittings were then used to determine the effect of B_0 on the contrast-to-noise ratio (CNR) between anoxia and three partial pressures of oxygen (15, 40, and 100 mmHg). In calculating the CNR, it was assumed that proton densities were equal, T_2 effects could be ignored, SNR increases linearly with B_0, and TR = 5 ms. The excitation angle was adjusted for optimal T_1 contrast as previously described.[48]

Results

MRS spectra were successfully acquired both *in vitro* (Fig. 2A) and *in vivo* (Fig. 2B). Multiple peaks were occasionally observed *in vivo*, possibly due to animal motion or uneven redistribution of the PFCE within the immunoisolation devices over time. R_1 was then determined using Equation (1) (Fig. 2C). The three-parameter equation that compensates for incomplete inversion was found to provide better fitting with smaller errors than a two-parameter equation. R_1 determination was found to be highly repeatable and fitting errors were typically <0.5% *in vitro* and <5% *in vivo*. The *in vivo* errors were found to be greater due to respiratory motion and poorer SNR.

To evaluate the potential MRS probes, R_1 data for each probe were fit to the multiparametric calibration equation previously described [Eq. (2)]. Probe characteristics and calibration results are summarized in Table 1. All probes had distinct advantages and weaknesses, making the choice of probe highly dependent on application. PFCE (chosen for our TEG studies) was confirmed to have a high number of equivalent nuclei (the number of nuclei in a molecule contributing to the MRS peak), high nuclear molarity (the number of nuclei [moles] contributing to an MRS peak per liter of compound), high oxygen sensitivity (change in R_1 with pO_2), high temperature sensitivity (change in R_1 with temperature), and high anoxic R_1 (fast relaxation without oxygen).

PFCE was then incorporated into TEGs and the R_1 was again found to be directly proportional to pO_2 with the slope and intercept dependent on temperature (Fig. 3A). A multiparametric calibration equation containing R_1, pO_2, and temperature [Eq. (2)] was successfully extrapolated (Table 2).

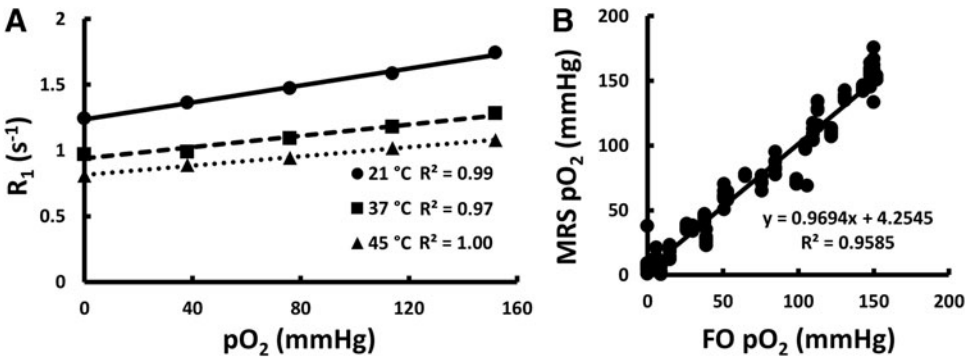

FIG. 3. *In vitro* oxygen calibration and validation using ^{19}F-MRS relaxometry and FO oxygen techniques. **(A)** Calibration of PFCE-loaded TEGs demonstrated that R_1 changes linearly with pO_2. The slope and intercept of the calibration line changed with temperature. These values were used to generate the multiparametric calibration coefficients. The error bars are contained within the markers. **(B)** Plotting ^{19}F-MRS against FO *in vitro* oxygen measurements showed a highly correlated relationship. These results validate the success of an accurate and reliable calibration (Pearson's R = 0.98, slope = 0.97, intercept = 4.3 mmHg). pO_2, oxygen partial pressure; TEG, tissue-engineered graft.

Table 2. Fitting Parameters Resulting from the Neat PFCE Calibration and the TEG Calibrations Used for the No DSO and DSO R_1 Measurements

	$A\ (s^{-1})$	$B\ (10^{-3}\ mmHg^{-1}\cdot s^{-1})$	$C\ (10^{-2}\ °C^{-1}\cdot s^{-1})$	$D\ (10^{-5}\ mmHg^{-1}\cdot °C^{-1}\cdot s^{-1})$
Neat	1.67 ± 0.01	3.64 ± 0.11	−1.97 ± 0.03	−3.80 ± 0.27
TEG, No DSO	1.65 ± 0.02	4.46 ± 0.19	−1.93 ± 0.05	−5.67 ± 0.53
TEG, DSO	1.66 ± 0.03	3.85 ± 0.06	−1.98 ± 0.08	−4.62 ± 0.16

DSO, delivery of supplemental oxygen; TEG, tissue-engineered graft.

^{19}F-MRS oxygen measurements correlated well ($p < 0.0001$) with FO oxygen measurements *in vitro* (Fig. 3B). These data validate ^{19}F-MRS as an accurate and reliable measurement technique *in vitro*.

In vivo validation using simultaneous FO and ^{19}F-MRS techniques for measuring pO_2 within implanted TEGs showed that FO probes consistently measured significantly higher oxygen levels than ^{19}F-MRS when compared using a two-tailed, paired Student's *t*-test (Fig. 4). The pO_2s measured with the FO oxygen probe were higher than ^{19}F-MRS measurements, but all measurements indicated a hypoxic or anoxic condition *in vivo*. The variability of FO oxygen measurements was found to be greater than ^{19}F-MRS measurements.

Oxygen gas was directly supplied to a subset of *in vivo* TEGs ($N = 3$) to ensure that ^{19}F-MRS could accurately detect a local increase in oxygenation. It was observed that TEGs with DSO had significantly higher pO_2s ($p < 0.0001$), as expected, with the supplemental oxygen increasing the TEG pO_2 from 39 ± 10 to 532 ± 35 mmHg as measured with ^{19}F-MRS. With the cessation of DSO, TEG pO_2 returned to the hypoxic levels previously seen without oxygen delivery (26 ± 22 mmHg; Fig. 5).

To compare our PFCE calibration results to other published values and evaluate the effect of B_0 on ^{19}F-MRS relaxometry for the measurement of pO_2, a comprehensive literature review was conducted. Eleven publications reporting information on PFCE R_1 oxygen sensitivity were identified.[28,30–36,38–40] One was excluded for inconsistent reporting of data[38] and another was excluded for results that differed from other reported data by several standard deviations,[40] leaving eleven reported calibrations[28,30–36,39] that were combined with our data for analysis. Oxygen sensitivity decreased (-6.39×10^{-5} $mmHg^{-1}\cdot s^{-1}$/T; Pearson's $R = -0.53$; Fig. 6A), anoxic R_1 increased (3.74×10^{-2} s^{-1}/T; Pearson's $R = 0.89$; Fig. 6B), and calculated oxygen CNR increased (Fig. 6C) with increasing B_0. Only three additional publications reported the R_1 temperature sensitivity of PFCE,[28,30,35] which prevented a meaningful analysis.

Discussion

Accurate oxygen measurements are critical to the development of TEGs for the treatment of diabetes and other diseases. Traditional sensors for oxygen measurement *in vivo* use polarographic needle or FO fluorescence-quenching probes. These traditional probes are invasive, often inaccurate, and only provide a single-point measurement at the tip of the probe itself, and, therefore, multiple mechanically disruptive measurements are required to obtain an average pO_2 measurement with small errors. This work demonstrates a method for noninvasive oxygen measurements within TEGs *in vivo* using MRS that overcomes many of these limitations, and offers an accurate, noninvasive, and temperature-compensating technique for TEG pO_2 measurements *in vivo*.

Our methods were optimized and adapted for measurements within macroencapsulated TEGs at ultra-high-field 16.4 T MRS to maximize signal intensities. We examined a number of potential oxygen probes and found that PFCE

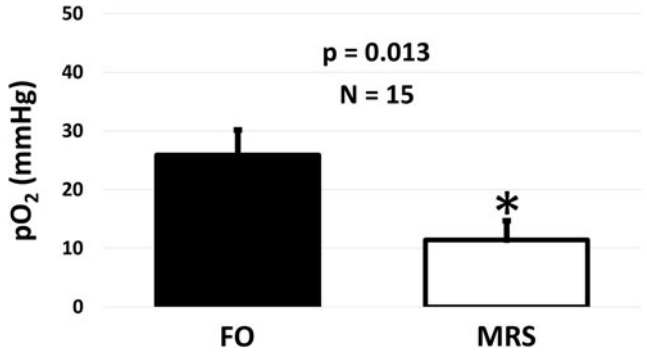

FIG. 4. Average *in vivo* pO_2 measured in implanted TEGs over 29 days using FO and ^{19}F-MRS techniques. Oxygen levels measured with both methods were less than venous blood pO_2 (40 mmHg), but there was a significant difference between methods with the FO probes measuring an average of 14 ± 6 mmHg higher than ^{19}F-MRS (*indicates significant difference $p < 0.05$).

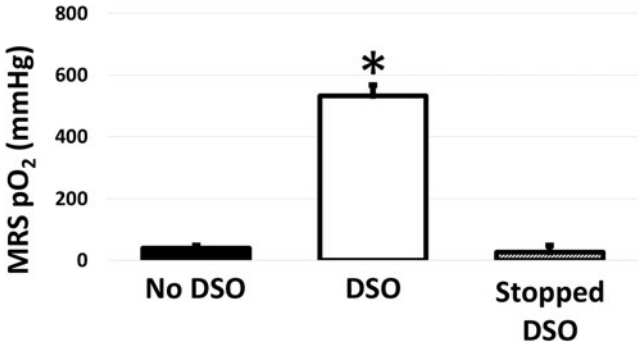

FIG. 5. *In vivo* pO_2 in implanted TEGs without DSO, with DSO, and after DSO was stopped as measured noninvasively with ^{19}F-MRS. DSO increased pO_2 in implanted TEGs. After DSO was discontinued, the reassessed pO_2 showed a return to low pO_2 previously seen without oxygen delivery. (*indicates a significant difference, $p < 0.0001$, when compared to the No DSO and Stopped DSO conditions). DSO, delivery of supplemental oxygen.

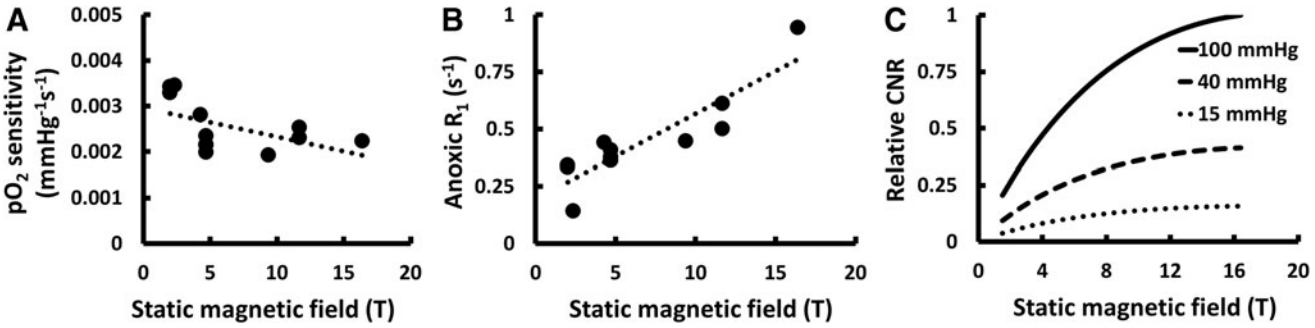

FIG. 6. Predicted changes in oxygen sensitivity, anoxic R_1, and theoretical oxygen CNR in an optimized gradient-echo image as a function of static magnetic field strength in Tesla (T) resulting from an analysis of our measurements combined with previously reported measurements. It was found that **(A)** oxygen sensitivity decreases, **(B)** anoxic R_1 increases, and **(C)** theoretical oxygen CNR in an optimized gradient-echo image increases with increasing static magnetic field strength. When transitioning from 1.5 to 16.4 T, the results predict a 33% decrease in oxygen sensitivity at 37°C, a 223% increase in anoxic R_1, and a 387% increase in CNR between 0 and 100 mmHg. CNR, contrast-to-noise ratio.

offers the best combination of high oxygen sensitivity, high nuclear molarity, and reported biocompatibility. Our data also demonstrate the sensitivity of R_1 to both oxygen and temperature. Additionally, the oxygen sensitivity of the probes were found to be dependent on temperature through Henry's law, necessitating that accurate MRS oxygen measurement techniques address this multiparametric physical nature. Controlling and measuring the temperature of an implanted oxygen probe is technically challenging, but due to the high sensitivity of MRS relaxation rates to both oxygen and temperature, temperature must be considered to measure pO_2 accurately and precisely.

To account for the effects of both oxygen and temperature on R_1, we used a multiparametric oxygen and temperature calibration using acellular TEGs loaded with a PFCE-impregnated plasma-gel matrix. High accuracy and precision in calibration were achieved by measuring R_1 using a surface coil, a standard inversion recovery pulse sequence with adiabatic pulses, and a three-parameter fit accounting for incomplete inversion. These measurements correlated well with measurements from an FO oxygen probe, suggesting that our MRS technique could reliably measure the pO_2 of *in vitro* samples with a high level of accuracy. Despite these complex calibrations, the *in vivo* oxygen measurements were still susceptible to errors in temperature measurement, and MRS methods for *in vivo* oximetry would greatly benefit from improved temperature measurement techniques, especially if the temperature measurements could be localized to the area of interest. An MRS method to locally measure temperature *in vivo* would be an ideal complement to MRS oximetry, and development in this area would greatly improve the sensitivity and accuracy of the described methods.

Our technique was validated *in vivo* with a series of rats implanted with TEGs that were modified with the addition of an access port to allow for insertion of an FO oxygen probe. This modification allowed for simultaneous pO_2 measurements using FO and MRS at various time points. A paired comparison between FO and MRS oxygen measurements indicated a significant difference in the measured *in vivo* pO_2 within implanted TEGs. While this difference is significant, both measurement techniques confirm a hypoxic oxygen level within the TEG *in vivo*. The disparity is due to critical differences between the FO and MRS methods. The FO oxygen probe provides a single-point measurement of pO_2 within the TEG, while MRS provides a volume-averaged measurement of the internal pO_2. This difference makes the FO probe method susceptible to local variabilities in oxygen levels, and probe placement is critical for measurements with FO probes. It is also important to note that the FO probe requires invasive intrusion into the TEG itself to obtain an oxygen measurement. The probe was inserted into the central compartment of the TEG, and this disturbs the matrix within the TEG. The FO probe is also likely introducing oxygen to the TEG during the insertion process, as it will be acclimated to atmospheric pO_2 and opens access to the external environment during the insertion procedure, which will likely contribute to measurement error. These likely contributed to the measurements with the FO oxygen probe having higher standard deviations when compared to the MRS technique. Despite the differences observed with these *in vivo* studies, MRS was found to provide reliable and reproducible measurements of internal TEG pO_2, and offers significant advantages over traditional invasive pO_2 measurement techniques.

For further confirmation of MRS pO_2 measurement techniques *in vivo*, the macroencapsulation device was modified to allow for continuous DSO to the TEG *in vivo*. MRS pO_2 measurements suggest a dramatic increase in local pO_2 in the TEGs with DSO. The results of these preliminary studies prove that MRS oxygen measurements can be used to measure the pO_2 of therapeutically relevant macroencapsulated TEGs *in vivo*. These measurements can be used to optimize these types of interventions, and to determine the optimal parameters for DSO.

The literature review clearly demonstrates that MRS relaxometry can be successfully applied to measure pO_2 at a variety of B_0, but that ultra-high-field is often advantageous for MRS pO_2 measurements. While our review suggests the oxygen sensitivities of MRS probes decrease with increasing B_0, there is a larger increase in SNR (and CNR) due to the increasing field and increase in R_1. For example, when increasing from 1.5 to 16.4 T, oxygen sensitivity decreases by a factor of 1.5 at 37°C, but the anoxic R_1 increases by a factor of 3.2 and the CNR between anoxia and 100 mmHg increases by a factor of 4.9.

In conclusion, these studies confirm that MRS can be an accurate and noninvasive technique to monitor TEG pO_2 for

long durations postimplantation. A multiparametric calibration was successfully developed to compensate for the temperature variability that is encountered during measurements, and this method improved the measurements of pO_2. Rigorous validations of our MRS technique with FO probes both *in vitro* and *in vivo* confirmed reliable measurements of internal TEG pO_2, and that this method can detect both natural physiological changes in the oxygen environment and interventional changes such as DSO. This technique will be a valuable tool to study the natural progression of oxygenation within implanted TEGs and to evaluate the success of DSO for increasing the internal pO_2 of implanted TEGs.

Acknowledgments

This work was supported in part by the Minnesota Lions Diabetes Foundation, the Schott Family Foundation, the Schulze Family Foundation, JDRF 5-2013-141, and NIH grants P41 EB015894 and S10 RR025031. The authors would like to thank all members of the Center for Magnetic Resonance Research for their thoughtful discussions, especially Drs. Bruce Hammer and Louis Kidder. Additional thanks to Jody Janecek, Dr. Leah Steyn, and Jessica Einstein.

Disclosure Statement

No competing financial interests exist.

References

1. Ludwig, B., Reichel, A., Steffen, A., Zimerman, B., Schally, A.V.V., Block, N.L.L., *et al.* Transplantation of human islets without immunosuppression. Proc Natl Acad Sci **110,** 19054, 2013.
2. Colton, C.K. Oxygen supply to encapsulated therapeutic cells. Adv Drug Deliv Rev **67,** 93, 2014.
3. Yang, H.K., and Yoon, K.-H. Current status of encapsulated islet transplantation. J Diabetes Complications **29,** 1, 2015.
4. Iacovacci, V., Ricotti, L., Menciassi, A., and Dario, P. The bioartificial pancreas (BAP): biological, chemical and engineering challenges. Biochem Pharmacol **100,** 12, 2016.
5. Weir, G.C. Islet encapsulation: advances and obstacles. Diabetologia **56,** 1458, 2013.
6. Scharp, D.W., and Marchetti, P. Encapsulated islets for diabetes therapy: history, current progress, and critical issues requiring solution. Adv Drug Deliv Rev **67,** 35, 2014.
7. Emamaullee, J.A., and Shapiro, A.M.J. Factors influencing the loss of β-cell mass in islet transplantation. Cell Transplant **16,** 1, 2007.
8. Suszynski, T.M., Avgoustiniatos, E.S., and Papas, K.K. Intraportal islet oxygenation. J Diabetes Sci Technol **8,** 575, 2014.
9. Ahearn, A.J., Parekh, J.R., and Posselt, A.M. Islet transplantation for Type 1 diabetes: where are we now? Expert Rev Clin Immunol **11,** 59, 2015.
10. Plesner, A., and Verchere, C.B. Advances and challenges in islet transplantation: islet procurement rates and lessons learned from suboptimal islet transplantation. J Transplant **2011,** 1, 2011.
11. Papas, K.K., Avgoustiniatos, E.S., and Suszynski, T.M. Effect of oxygen supply on the size of implantable islet-containing encapsulation devices. Panminerva Med **58,** 72, 2016.
12. Dionne, K.E., Colton, C.K., and Yarmush, M.L. Effect of oxygen on isolated pancreatic tissue. ASAIO Trans **35,** 739, 1989.
13. Papas, K.K., Avgoustiniatos, E.S., Tempelman, L.A., Weir, G.C., Colton, C.K., Pisania, A., *et al.* High-density culture of human islets on top of silicone rubber membranes. Transplant Proc **37,** 3412, 2005.
14. Barkai, U., Weir, G.C., Colton, C.K., Ludwig, B., Bornstein, S.R., Brendel, M.D., *et al.* Enhanced oxygen supply improves islet viability in a new bioartificial pancreas. Cell Transplant **22,** 1463, 2013.
15. Evron, Y., Zimermann, B., Ludwig, B., Barkai, U., Colton, C., Weir, G., *et al.* Oxygen supply by photosynthesis to an implantable islet cell device. Horm Metab Res **47,** 24, 2014.
16. Suszynski, T.M., Avgoustiniatos, E.S., Stein, S.A., Falde, E.J., Hammer, B.E., and Papas, K.K. Assessment of tissue-engineered islet graft viability by fluorine magnetic resonance spectroscopy. Transplant Proc **43,** 3221, 2011.
17. Suszynski, T.M. Tissue-Engineered Islet Graft Design and Assessment. Minneapolis, MN: University of Minnesota, 2012.
18. Zhao, D., Jiang. L.P., and Mason, R. Measuring changes in tumor oxygenation. Methods Enzymol **386,** 378, 2004.
19. Vikram, D.S., Zweier, J.L., and Kuppusamy, P. Methods for noninvasive imaging of tissue hypoxia. Antioxid Redox Signal **9,** 1745, 2007.
20. Shaw, A.D., Li, Z., Thomas, Z., and Stevens, C.W. Assessment of tissue oxygen tension: comparison of dynamic fluorescence quenching and polarographic electrode technique. Crit Care **6,** 76, 2001.
21. Amao, Y. Probes and polymers for optical sensing of oxygen. Microchim Acta **143,** 1, 2003.
22. Shao, Q., and Ashkenazi, S. Photoacoustic lifetime imaging for direct in vivo tissue oxygen monitoring. J Biomed Opt **20,** 36004, 2015.
23. Gordji-Nejad, A., Möllenhoff, K., Oros-Peusquens, A.M., Pillai, D.R., and Shah, N.J. Characterizing cerebral oxygen metabolism employing oxygen-17 MRI/MRS at high fields. MAGMA **27,** 81, 2014.
24. Parhami, P., and Fung, B. Fluorine-19 relaxation study of perfluoro chemicals as oxygen carriers. J Phys Chem **87,** 1928, 1983.
25. Ruiz-Cabello, J., Barnett, B.P., Bottomley, P.A., and Bulte, J.W.M. Fluorine (19F) MRS and MRI in biomedicine. NMR Biomed **24,** 114, 2011.
26. Riess, J.G. Understanding the fundamentals of perfluorocarbons and perfluorocarbon emulsions relevant to in vivo oxygen delivery. Artif Cells Blood Substit Immobil Biotechnol **33,** 47, 2005.
27. Mason, R.P., Shukla, H., and Antich, P.P. In vivo oxygen tension and temperature: simultaneous determination using 19F NMR spectroscopy of perfluorocarbon. Magn Reson Med **29,** 296, 1993.
28. Dardzinski, B.J., and Sotak, C.H. Rapid tissue oxygen tension mapping using 19F inversion-recovery echo-planar imaging of perfluoro-15-crown-5-ether. Magn Reson Med **32,** 88, 1994.
29. Shukla, H.P., Mason, R.P., Woessner, D.E., and Antich, P.P. A comparison of three commercial perfluorocarbon emulsions as high-field 19F NMR probes of oxygen tension and temperature. J Magn Reson Ser B 131, 1995.
30. Helmer, K.G., Han, S., and Sotak, C.H. On the correlation between the water diffusion coefficient and oxygen tension in RIF-1 tumors. NMR Biomed **11,** 120, 1998.

31. van der Sanden, B.P.J., Heerschap, A., Simonetti, A.W., Rijken, P.F.J.W., Peters, H.P.W., Stuben, G., *et al.* Characterization and validation of noninvasive oxygen tension measurements in human glioma xenografts by 19F-MR relaxometry. Int J Radiat Oncol **44,** 649, 1999.
32. Duong, T.Q., and Kim, S.G. In vivo MR measurements of regional arterial and venous blood volume fractions in intact rat brain. Magn Reson Med **43,** 393, 2000.
33. Duong, T.Q., Iadecola, C., and Kim, S.G. Effect of hyperoxia, hypercapnia, and hypoxia on cerebral interstitial oxygen tension and cerebral blood flow. Magn Reson Med **45,** 61, 2001.
34. Fan, X., River, J.N., Zamora, M., Al-Hallaq, H.A., and Karczmar, G.S. Effect of carbogen on tumor oxygenation: combined fluorine-19 and proton MRI measurements. Int J Radiat Oncol Biol Phys **54,** 1202, 2002.
35. McNab, J.A., Yung, A.C., and Kozlowski, P. Tissue oxygen tension measurements in the Shionogi model of prostate cancer using 19F MRS and MRI. MAGMA **17,** 288, 2004.
36. Gross, J.D.D., Long, R.C.R.C., Constantinidis, I., and Sambanis, A. Monitoring of dissolved oxygen and cellular bioenergetics within a pancreatic substitute. Biotechnol Bioeng **98,** 261, 2007.
37. Kodibagkar, V.D., Wang, X., and Mason, R.P. Physical principles of quantitative nuclear magnetic resonance oximetry. Front Biosci **13,** 1371, 2008.
38. Goh, F., and Sambanis, A. In vivo noninvasive monitoring of dissolved oxygen concentration within an implanted tissue-engineered pancreatic construct. Tissue Eng Part C Methods **17,** 887, 2011.
39. Goh, F. The use of perfluorocarbons in encapsulated cell systems: their effect on cell viability and function and their use in noninvasively monitoring the cellular microenvironment. Atlanta, GA: Georgia Institute of Technology, 2011.
40. Mignion, L., Magat, J., Schakman, O., Marbaix, E., Gallez, B., and Jordan, B.F. Hexafluorobenzene in comparison with perfluoro-15-crown-5-ether for repeated monitoring of oxygenation using 19F MRI in a mouse model. Magn Reson Med **69,** 248, 2013.
41. Kodibagkar, V.D., Cui, W., Merritt, M.E., and Mason, R.P. Novel 1H NMR approach to quantitative tissue oximetry using hexamethyldisiloxane. Magn Reson Med **55,** 743, 2006.
42. Nöth, U., Gröhn, P., Jork, A., Zimmermann, U., Haase, A., and Lutz, J. 19F-MRI in vivo determination of the partial oxygen pressure in perfluorocarbon-loaded alginate capsules implanted into the peritoneal cavity and different tissues. Magn Reson Med **42,** 1039, 1999.
43. Zimmermann, U., Nöth, U., Gröhn, P., Jork, A., Ulrichs, K., Lutz, J., *et al.* Non-invasive evaluation of the location, the functional integrity and the oxygen supply of implants: ^{19}F nuclear magnetic resonance imaging of perfluorocarbon-loaded BA^{2+}-alginate beads. Artif Cells Blood Substit Immobil Biotechnol **28,** 129, 2000.
44. Goh, F., Long, R., Simpson, N., and Sambanis, A. Dual perfluorocarbon method to noninvasively monitor dissolved oxygen concentration in tissue engineered constructs in vitro and in vivo. Biotechnol Prog **27,** 1115, 2011.
45. Fung, B.M. Selective detection of multiplets via double quantum coherence: A19F NMR study of perfluorodecalin. Org Magn Reson **21,** 397, 1983.
46. Bernassau, J-M., and Hyafil, F. Choice of delay time sequence in spin-lattice relaxation time measurements by inversion-recovery. J Magn Reson **40,** 245, 1980.
47. Weiss, G.H., and Ferretti, J.A. Optimal design of relaxation time experiments. Prog Nucl Magn Reson Spectrosc **20,** 317, 1988.
48. Buxton, R., Edelman, R., Rosen, B., Wismer, G., and Brady, T. Contrast in rapid MR imaging: T1- and T2-weighted imaging. J Comput Assist Tomogr **11,** 7, 1987.

Address correspondence to:
Michael Garwood, PhD
Department of Radiology
Center for Magnetic Resonance Research
University of Minnesota
Minneapolis, MN 55455

E-mail: gar@umn.edu

Received: March 21, 2016
Accepted: September 26, 2016
Online Publication Date: November 14, 2016